Low-temperature preparation of GaN-SiO_2 interfaces with low defect density. II. Remote plasma-assisted oxidation of GaN and nitrogen incorporation

Choelhwyi Bae and Gerald Lucovsky[a)]
Department of Physics, Materials Science and Engineering, and Electrical and Computer Engineering, North Carolina State University, Raleigh, North Carolina 27695-8202

(Received 27 August 2003; accepted 23 August 2004; published 20 October 2004)

Low-temperature remote plasma-assisted oxidation and nitridation processes for interface formation and passivation have been extended from Si and SiC to GaN. The initial oxidation kinetics and chemical composition of thin interfacial oxide were determined from analysis of on-line Auger electron spectroscopy features associated with Ga, N, and O. The plasma-assisted oxidation process is self-limiting with power-law kinetics similar to those for the plasma-assisted oxidation of Si and SiC. Oxidation using O_2/He plasma forms nearly pure GaO_x, and oxidation using 1% N_2O in N_2 forms GaO_xN_y with small nitrogen content, ~4–7 at. %. The interface and dielectric layer quality was investigated using fabricated GaN metal-oxide-semiconductor capacitors. The lowest density of interface states was achieved with a two-step plasma-assisted oxidation and nitridation process before SiO_2 deposition. © *2004 American Vacuum Society.* [DOI: 10.1116/1.1807411]

I. INTRODUCTION

GaN has received great attention for applications in optoelectronic and electronic devices due to its direct and wide band-gap properties.[1] Studies of the GaN metal-insulator-semiconductor system have focused on reducing the interface state density (D_{it}), and these efforts can be classified into four groups: (i) deposited amorphous SiO_2,[2] Si_3N_4,[3] and high-*k* Ta_2O_5;[4] (ii) epitaxially grown AlN,[5] Gd_2O_3,[6] and $Ga_2O_3(Gd_2O_3)$;[7] (iii) native oxide by oxidation of GaN surface using thermal,[8,9] photoelectrochemical,[10–12] remote O_2/He plasma,[13] and N_2O/He plasma methods;[14] and (iv) gate stacks such as $SiO_2/Si_3N_4/SiO_2$ (ONO).[15]

In previous studies,[16,17] device-quality Si-SiO_2 interfaces and dielectric bulk film of SiO_2 were prepared using a two-step process: (i) remote plasma-assisted oxidation (RPAO) to form a superficially thin interfacial oxide (~0.6 nm) and (ii) remote plasma-enhanced chemical vapor deposition to deposit the SiO_2 film. The same processing steps have been applied to SiC-SiO_2 (Ref. 18) and GaN-SiO_2 interfaces.[13] This present work is concerned with remote plasma-assisted oxidation of GaN for the independent control of GaN-GaO_x (or GaO_xN_y) interface formation and dielectric film deposition. Three important aspects in preparing thin RPAO oxide, with a composition close to Ga_2O_3 or $x \sim 1.5$, of GaN are (i) RPAO oxide thickness, (ii) RPAO source gas, and (iii) incorporated nitrogen content in RPAO oxide. Pure Ga_2O_3 showed high leakage current and did not passivate the GaAs (Refs. 19 and 20) and SiGe (Ref. 21) surface due to oxygen vacancies and/or a small amount of reduced Ga in the films. Codeposition of electropositive rare-earth elements, such as Gd and Y, was suggested for minimizing oxygen vacancies and stabilizing Ga in the fully oxidized 3+ states. When the RPAO process is performed to prevent parasitic subcutaneous oxidation of the GaN surface, which occurs during SiO_2 film deposition,[22] RPAO oxide should be carefully controlled as a superficially thin (or several monolayer) oxide. Considering the nitrogen-incorporated Si-SiO_2 and Si-high-*k* interface, nitridation of thin RPAO oxide makes an important impact on the GaN-GaO_x (or RPAO oxide) interface.

In this study, the RPAO process of the GaN surface using O_2, N_2O, and 10% (or 1%) N_2O in N_2 source gas has been investigated. The initial oxidation kinetics and chemical composition of thin RPAO oxide were determined from analysis of on-line Auger electron spectroscopy (AES) features associated with Ga, N, and O. Also, remote plasma-assisted nitridation of the RPAO oxide is discussed. The interface and dielectric layer quality was investigated using fabricated GaN metal-oxide-semiconductor (MOS) capacitors.

II. EXPERIMENT

The epitaxial GaN (0001) layer was grown directly on the *c* plane of sapphire by hydride vapor-phase epitaxy (Technologies and Devices International, Inc.). Silicon was used as a *n*-type dopant, and the thickness of the GaN epitaxial layer was 5 μm. The as-grown GaN layer had an electron concentration of $5-10\times10^{17}$ cm^{-3}. The as-received 50-mm GaN epiwafer on sapphire was cut into four pieces and degreased for 10 min in each of three organic solvents (trichloroethylene, acetone, methanol). After the wet-chemical treatment using 1:1:5 $NH_4OH:H_2O_2:H_2O$ solution at ~80 °C and followed etching in 1:5 $NH_4OH:H_2O$ solutions at ~80 °C, GaN samples were loaded into a multichamber system,[17] which provided separate remote plasma-assisted process and on-line AES measurement. Prior to the RPAO process, the as-loaded GaN sample was exposed to reactive species from a remote N_2/He discharge at 0.02 Torr.[22] Then, the *in situ*

[a)]Author to whom correspondence should be addressed; electronic mail: gerry_lucovsky@ncsu.edu

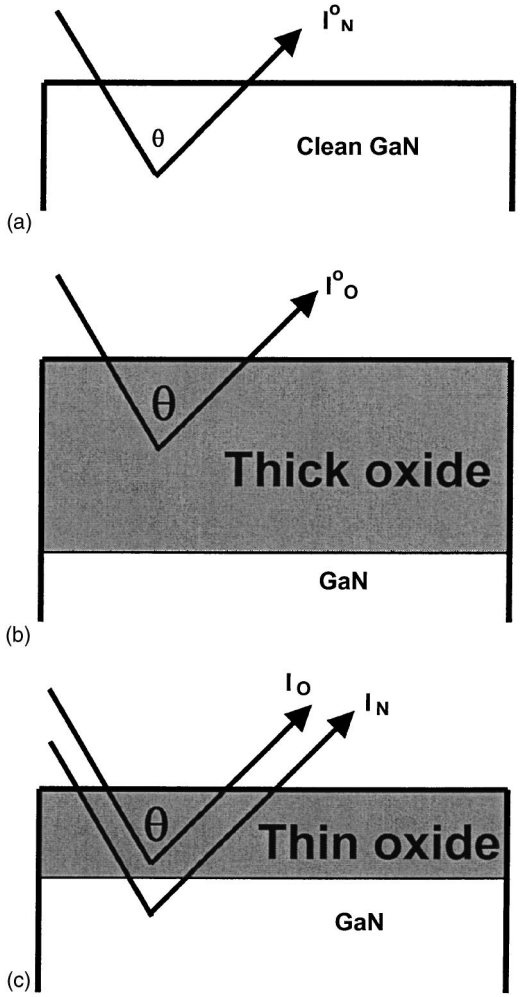

FIG. 1. Schematic representation of three samples: (a) clean GaN substrate; (b) thick pure GaO_x; and (c) thin pure GaO_x on GaN substrate. I^o_N (or I_N) is N *KLL* Auger electron intensity from the clean GaN substrate (or from the GaN substrate with thin oxide). I^o_O (or I_O) is O *KLL* Auger electron intensity from the thick GaO_x layer (or from the thin GaO_x layer).

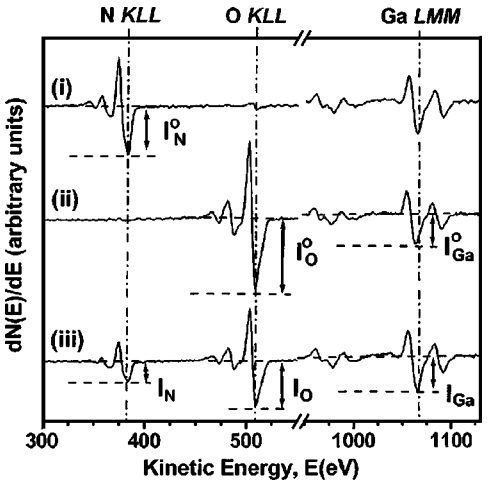

FIG. 2. Differential AES spectra from (i) clean GaN, (ii) thick RPAO oxide, and (iii) thin RPAO oxide on GaN substrate. N_2/He-plasma-cleaned GaN sample (300 °C, 0.02 Torr, 30 W, and 15 min) was used as a reference sample for a clean GaN, and O_2/He-plasma-oxidized GaN sample (300 °C, 0.3 Torr, 60 W, and 30 min) was used as a reference sample for a thick pure GaO_x.

cleaned GaN surface was oxidized by the RPAO process at 0.3 Torr using O_2, N_2O, and N_2O in N_2 source gas. The processing temperature was 250°–300 °C, and rf power was 30–60 W at 13.56 MHz. For O_2 (or N_2O)/He plasma oxidation, O_2 (or N_2O)/He discharge was used at flows of 20 sccm O_2 (or N_2O) and 200 sccm He. To check for further nitrogen incorporation, GaN samples were exposed to N_2O/N_2/He plasma using (i) 10% N_2O in N_2 (6/54/200 $N_2O:N_2$:He) and (ii) 1% N_2O in N_2 (60/200 1% N_2O in N_2:He) source gas. For the nitridation process, a thick oxide formed by the RPAO process was exposed to reactive species from a remote N_2/He discharge at 0.3 Torr. The processing temperature was 300 °C, and rf power was 30 W at 13.56 MHz. The experimental procedure was to alternate AES measurements using a 3-keV electron beam with the remote plasma-assisted process, i.e., interrupted processing and AES analysis cycles.

For the fabrication of GaN MOS capacitors, the RPAO process was performed on the wet-chemical-treated GaN surface to form an RPAO oxide of ~1.0 (or ~1.6) nm, and the RPECVD process was performed for 12 min to deposit SiO_2 of ~40 nm. After gate dielectric insulator deposition, the sample was rapid-thermal annealed at ~900 °C for 30 s in Ar atmosphere. A 300-nm Al layer was evaporated and defined by the conventional lithography process. Postmetallization annealing was performed at 400 °C for 30 min in forming gas (N_2/H_2). The electrical properties of GaN MOS capacitors were investigated using an HP 4284A (precision inductance-capacitance-resistance meter). The area of the device being tested was 4×10^{-4} cm^2.

III. RESULTS AND DISCUSSION

A. Oxidation rate using on-line AES

The kinetics of the RPAO process on the GaN surface are determined by using AES analysis, and the thin oxide thickness t_{ox} (nm) can be fitted by an empirical power-law function of the form $t_{ox}=\tau_o t^{\beta}$, where t is the oxidation time (min), and τ_o and β are fitting parameters. Assuming negligible nitrogen content in the RPAO oxide or GaO_x with $x\sim1.5$, N *KLL*, and O *KLL* AES intensities are given by (Ref. 23 and references therein)

$$I_N = I^o_N \exp(-t_{ox}/\lambda_N), \tag{1}$$

$$I_O = I^o_O[1-\exp(-t_{ox}/\lambda_O)], \tag{2}$$

where I_N=N *KLL* Auger electron intensity from the GaN substrate, I^o_N=N *KLL* Auger electron intensity from the clean GaN substrate, λ_N=electron escape depth for N, I_O=O *KLL* Auger electron intensity from the thin GaO_x layer, I^o_O=O *KLL* Auger electron intensity from the thick GaO_x layer, and λ_O=electron escape depth for O.

Figure 1 illustrates three samples: (a) clean GaN substrate; (b) thick pure GaO_x; and (c) thin pure GaO_x on GaN substrate. In this study, a N_2/He plasma-cleaned GaN sample

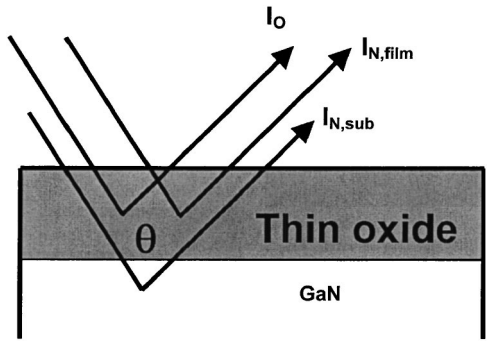

FIG. 3. Schematic representation of thin RPAO oxide, or GaO_xN_y with non-negligible nitrogen content, on GaN substrate. When the nitrogen content in the oxide is not negligible, total intensity of N *KLL* (I_N) consists of (i) intensity of N *KLL* from the substrate ($I_{N,sub}$) and (ii) intensity of N *KLL* from the oxide film ($I_{N,film}$).

(300 °C, 0.02 Torr, 30 W, and 15 min) was used as a clean GaN for I^o_N, and an O_2/He plasma-oxidized GaN sample (300 °C, 0.3 Torr, 60 W, and 30 min) was used as a thick pure GaO_x for I^o_O. The obtained value of I^o_N/I^o_O is ~0.65. Figure 2 shows AES spectra from: (i) clean GaN; (ii) thick RPAO oxide; and (iii) thin RPAO oxide on GaN substrate. To determine t_{ox}, Eqs. (1) and (2) are combined as in the following equation by assigning the same value of electron escape depth, $\lambda = 1.0$ nm, for both λ_N and λ_O:

$$t_{ox} = \lambda \ln\left(1 + \frac{I^o_N}{I^o_O} \times \frac{I_O}{I_N}\right). \quad (3)$$

To determine t_{ox} only using Eq. (2) without the assumption of negligible nitrogen content in the oxide, I_O in each AES spectra is normalized by the Ga *LMM* Auger electron intensity (I_{Ga}). The normalized intensity of O *KLL* from the thick RPAO oxide layer (I^o_O/I^o_{Ga}) is 2.35. Then, the oxide thickness is given by

$$t_{ox} = -\lambda_O \ln\left(1 - \frac{I^o_{Ga}}{I^o_O} \times \frac{I_O}{I_{Ga}}\right). \quad (4)$$

When the nitrogen content in the RPAO oxide is not negligible, the total intensity of N *KLL* (I_N) consists of the (i) intensity of N *KLL* from the substrate ($I_{N,sub}$) and (ii) intensity of N *KLL* from the oxide film ($I_{N,film}$), as shown in Fig. 3. In the initial stage of oxidation, $I_{N,film}$ is much smaller than $I_{N,sub}$ and can be ignored. As the thickness of the oxide film increases, $I_{N,sub}$ gradually reduces and becomes comparable to $I_{N,film}$. Thus, t_{ox} from Eq. (3) using I_O/I_N becomes smaller than t_{ox} from Eq. (4) using I_O/I_{Ga}.

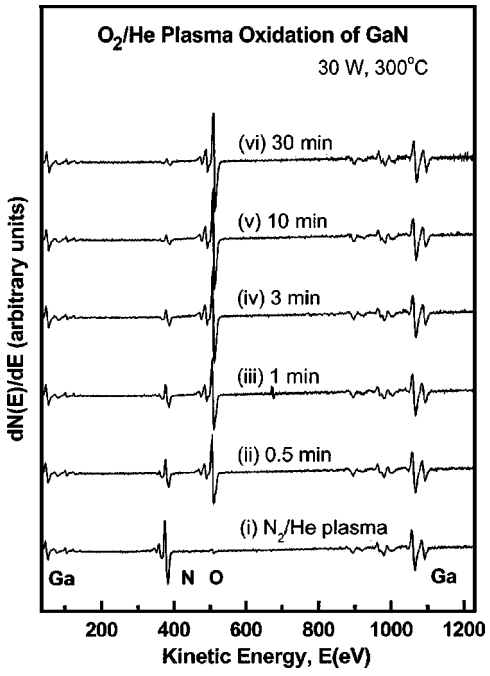

FIG. 4. Time evolution of differential AES spectra from (i) N_2/He-plasma-cleaned GaN sample and (ii)–(vi) O_2/He-plasma-oxidation processing of GaN surface for 0.5 to 30 min.

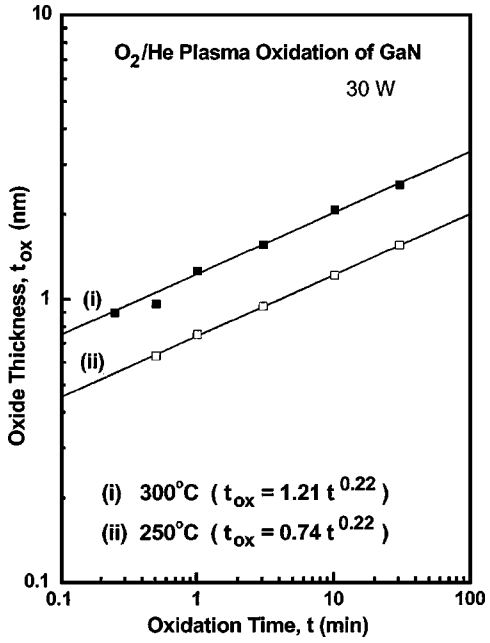

FIG. 5. Log-log plots of the oxide thickness (t_{ox}) as a function of oxidation time (t) for the RPAO process using O_2 source gas at 250° and 300 °C. The straight lines connecting the data points represent a power-law dependence, i.e., $t_{ox} = \tau_o t^{\beta}$, where τ_o and β are fitting parameters. The oxide thickness is determined from Eq. (3) using I_O/I_N, with an assumption of a homogeneous overlayer/substrate (GaO_x/GaN) system.

B. Remote O_2/He plasma oxidation: Pure GaO_x/GaN system

Figure 4 shows the evolution over time of differential AES spectra for the RPAO process of a GaN sample using O_2 source gas at 300 °C with plasma power of 30 W. Although the Ga *LMM* (~1060.5 eV) feature shows a negligible change in strength as the oxidation proceeds, the N *KLL* (~377.5 eV) feature, which is mainly associated with N-Ga bonding in the GaN substrate, decreases in strength, and the O *KLL* (~505.5 eV) feature, which is mainly associated with O-Ga bonding in the thin oxide layer,

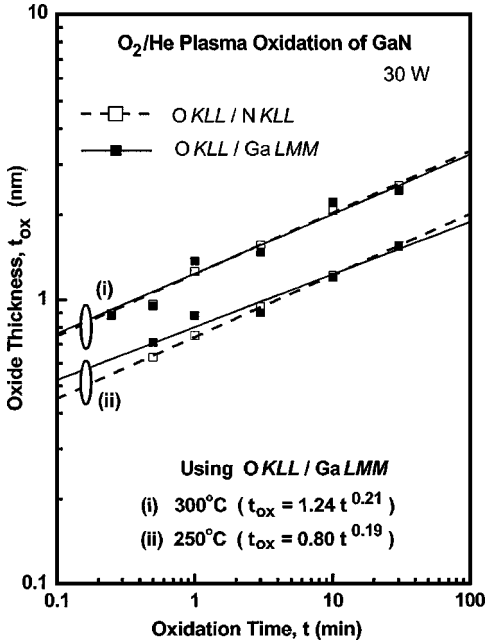

FIG. 6. Log-log plots of the oxide thickness (t_{ox}), determined from Eq. (4) using I_O/I_{Ga} and taking λ_O as 1.14 nm, as a function of oxidation time (t) for the same RPAO process shown in Fig. 5. The oxide thickness and fitting data shown in Fig. 5 are also included as references.

increases in strength. These changes in relative intensity of N *KLL* and O *KLL* are due to the increase of the oxide thickness with time.

Figure 5 shows log-log plots of the oxide thickness versus oxidation time for the RPAO process using O_2 gas source at 250° and 300 °C. The oxide thickness is determined using I_O/I_N. The relation of oxide thickness versus oxidation time can be fitted by the power-law function, $t_{ox}=\tau_0 t^{\beta}$, $t_{ox}=1.21t^{0.22}$ (300 °C) and $t_{ox}=0.74t^{0.22}$ (250 °C). The exponential constant β of the GaN oxidation (~0.22) is smaller than the corresponding exponential constant for Si (~0.28) (Ref. 17) and SiC (~0.40).[18] As shown in Fig. 6, the oxide thickness using I_O/I_{Ga} and taking λ_O as 1.14 nm showed good agreement with the oxide thickness using I_O/I_N. This result suggests that the chemical composition of the RPAO oxide using O_2 source gas is nearly pure GaO_x (or GaO_xN_y, with negligible y). In addition, the nearly nonexistent N *KLL* feature of the GaN sample oxidized at 60 W for 30 min, shown in Fig. 2, also indicates that the nitrogen content in the RPAO oxide is negligible. For this thick-oxide sample, the oxide thickness is determined as ~3.5 nm. Because the electron escape depth at 400–500 eV is ~1.0 nm, theoretically, the oxide thickness using N *KLL* and O *KLL* features can be estimated up to ~4.0 nm, at which point the AES signal (N *KLL*) from the substrate becomes too weak to measure. Therefore, power-law fitting with an approximation of a homogeneous overlayer/substrate (GaO_x/GaN) system is self-consistent.

Figure 7 displays the peak shift of nondifferentiated AES spectra as a function of oxidation time. As oxidation proceeds, the Ga *LMM* (~1060.5 eV) feature gradually shifts to lower energy. The gradual peak shift (~1.5 eV) of the

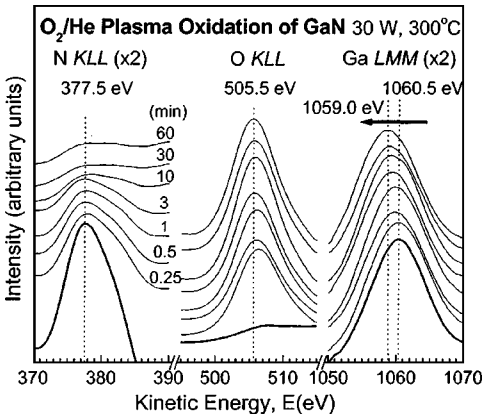

FIG. 7. Time evolution of nondifferential AES spectra from *in situ* N_2/He-plasma-cleaned GaN sample and O_2/He-plasma-oxidation processing of GaN surface for 0.25 to 60 min.

Ga *LMM* feature indicates that Ga–N bonds change to Ga–O bonds. Figure 8 indicates the relative change in composition of the oxidized GaN sample as a function of oxidation time, where [Ga], [O], and [N] are Ga, O, and N atomic fraction in the film (at. %), respectively (Ref. 23 and reference therein). AES intensities of each element are divided by the mean free paths to make the initial [Ga]/[N] ratio unity. Because AES intensities of Ga *LMM* and N *KLL* come from both the thin oxide layer and GaN substrate, the atomic fractions of each element determined are not the actual compositions of oxide film until the film grows to be a thick film (>4 nm). Figure 8 only indicates relative concentration changes of each element during the oxidation of GaN. Increasing the oxidation time, [N] changes from ~50 at. % to near zero as [O] changes from near zero to ~50 at. %, whereas [Ga] shows a negligible change from the initial concentration, ~50 at. %.

C. Remote N_2O/He (or N_2/N_2O/He) plasma oxidation: Nitrogen incorporation

To investigate nitrogen incorporation and the possible formation of gallium oxynitride film, GaN samples were ex-

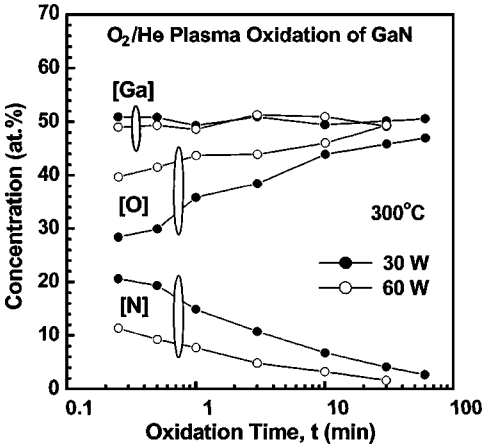

FIG. 8. Relative change in composition of GaO_x as a function of oxidation time, where [Ga], [O], and [N] are Ga, O, and N atomic fraction in the film (at. %), respectively.

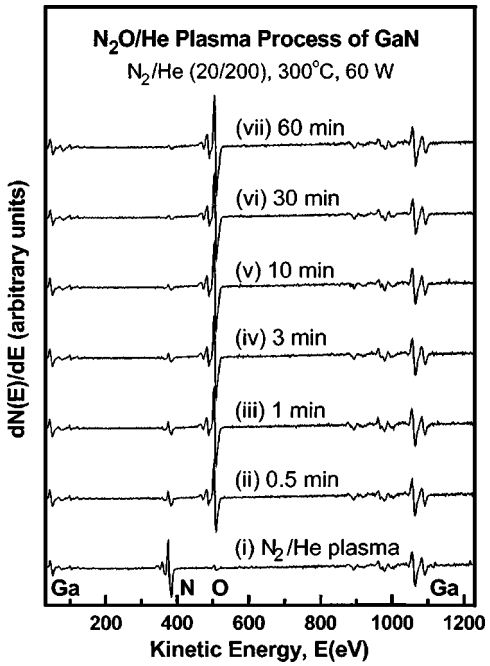

FIG. 9. Time evolution of differential AES spectra from (i) N_2/He-plasma-cleaned GaN sample and (ii)–(vii) N_2O/He-plasma oxidation processing of GaN surface for 0.5 to 60 min. The notation (20/200) in the figure refers to the flow rates of N_2O and He, respectively, in units of standard cubic centimeters per second (sccm).

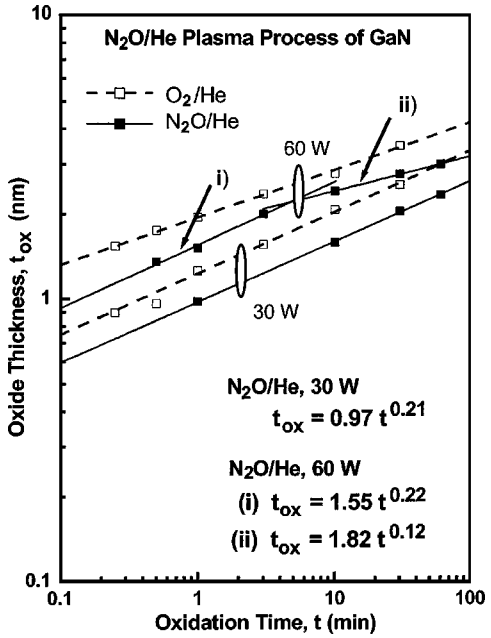

FIG. 10. Log-log plots of the oxide thickness (t_{ox}) as a function of oxidation time (t) for the RPAO process using N_2O source gas at 300 °C with 30 and 60 W. The oxide thickness is determined from Eq. (3) using I_O/I_N. The oxide thickness and fitting data using O_2 source gas are also included as references.

posed to N_2O/He plasma at 300 °C with plasma powers of 30 and 60 W. Figure 9 shows the evolution over time of differential AES spectra for the RPAO process of a GaN sample with 60 W. The changes in relative intensity of N *KLL* and O *KLL* are similar to those of oxidation using O_2 source gas, except the N *KLL* feature is slightly apparent. This observation indicates that N_2O/He plasma oxidation of the GaN surface also resulted in nearly pure GaO_x. The peak shift of nondifferentiated AES features from the oxidized GaN sample and the relative change in composition as a function of oxidation time were similar to the oxidation of GaN using O_2 source gas (not shown in figure).

Figure 10 shows log-log plots of the oxide thickness using I_O/I_N versus oxidation time and power-law fitting for the RPAO process using N_2O source gas at 300 °C with 30 and 60 W. Oxide thicknesses using I_O/I_N and fit data from O_2/He plasma oxidation with 30 and 60 W are included as references. In the cases of $t_{ox} < \sim 2.0$ nm, the growth rate for the N_2O/He process decreased as compared to that of the O_2/He plasma process with a similar exponential constant β. As the t_{ox} increased $> \sim 2.0$ nm, the oxidation rate for the N_2O process decreased. The growth rate for the N_2O/He process with 60 W was fitted by two different exponential constants with increasing oxidation time: (i) $t_{ox} = 1.55\ t^{0.22}$ up to 3 min and (ii) $t_{ox} = 1.82\ t^{0.12}$ for the extended oxidation time. This is attributed to the ignored $I_{N,film}$ in determining oxide thickness using I_O/I_N, and it also indicates that a small amount of nitrogen was incorporated into the RPAO oxide layer.

Figure 11 shows log-log plots of the oxide thickness versus oxidation time for the RPAO process using (i) 10% N_2O and (ii) 1% N_2O source gas. Oxide thickness was determined using I_O/I_N and I_O/I_{Ga}, respectively. Power-law fitting was performed for the oxide thickness using I_O/I_{Ga}. When t_{ox}

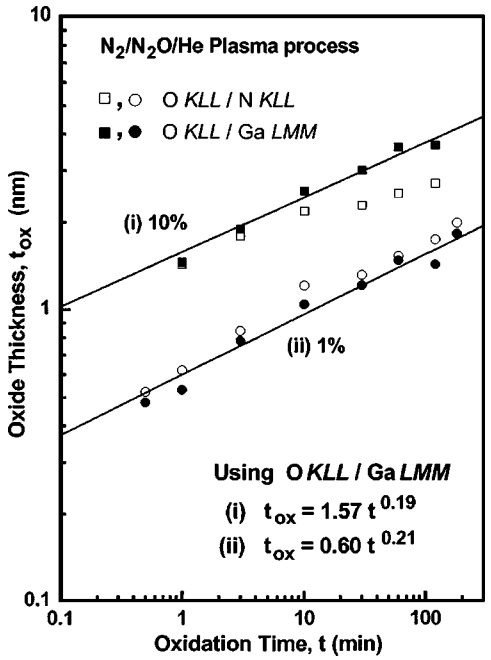

FIG. 11. Log-log plots of the oxide thickness (t_{ox}), determined from Eq. (4) using I_O/I_{Ga} and taking λ_O as 1.14 nm, as a function of oxidation time (t). The notation 10% and 1% in the figure refer to 10% N_2O in N_2 and 1% N_2O in N_2, respectively.

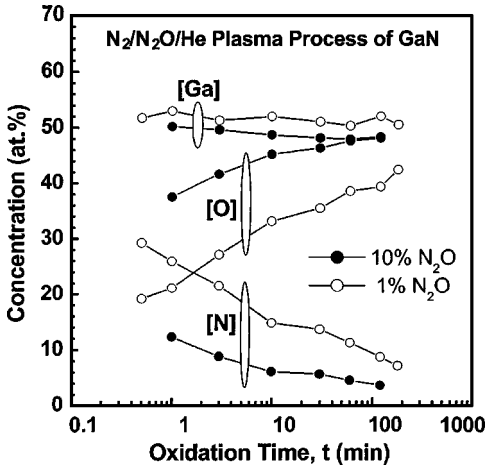

FIG. 12. Relative change in composition of an oxidized GaN sample as a function of oxidation time, where [Ga], [O], and [N] are Ga, O, and N atomic fraction in the film (at. %), respectively.

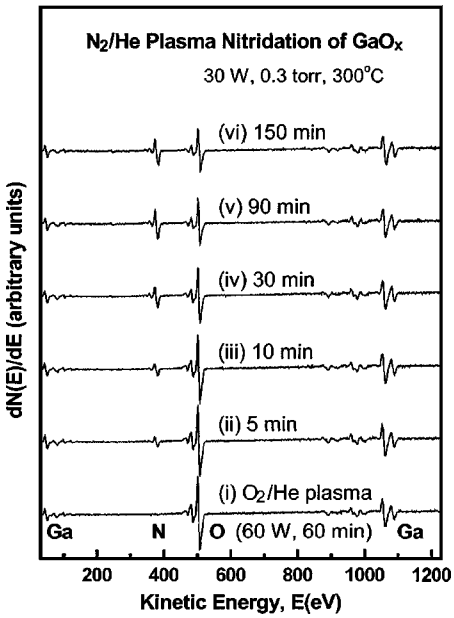

FIG. 13. Time evolution of differential AES spectra from (i) O_2/He-plasma-oxidized GaN sample (GaO_x, ~3.5 nm) and (ii)–(vi) N_2/He-plasma-nitridation processing of GaO_x for 5 to 150 min.

increased $>\sim 2.0$ nm, the oxide thickness using I_O/I_N shows deviation from the power-law fitting. This deviation confirms the nitrogen incorporation in the RPAO oxide layer, but indicates that the nitrogen incorporation was not significantly enhanced by increasing the N/O ratio in source gas. Figure 12 shows the relative change in composition of the oxidized GaN sample as a function of oxidation time. For the oxidized sample using 10% N_2O for 120 min, the value of [N], ~4 at. %, is obtained mainly from the oxide layer because the oxide thickness is $>\sim 3.5$ nm. For the sample using 1% N_2O for 180 min, the AES intensity of N *KLL* from the GaN substrate is not yet negligible. Thus, the incorporated nitrogen content in the sample using 1% N_2O will be ~4–7 at. %. Although other characterization methods are needed to obtain the exact value of the incorporated nitrogen content, the present result indicates that only a small amount of nitrogen was incorporated in the oxide during the RPAO process in the ranges of N/O in source gas that were studied.

D. Remote N_2/He plasma nitridation of GaO_x: Enhanced nitrogen incorporation

Figure 13 shows differential AES spectra for (i) the thick RPAO oxide (>3.5 nm) film prepared from O_2/He plasma oxidation of the GaN followed by (ii)–(vi) the exposure to N_2/He plasma for 5–150 min at 0.3 Torr. The intensity of N *KLL* increased as the exposure time to N_2/He plasma increased to 5–90 min, and it saturated with no significant spectral change for the extended nitridation time. By reoxidation using O_2/He plasma for 1 min, this increased intensity of the N *KLL* feature was reduced to the initial values of the RPAO oxide film before the exposure to N_2/He plasma. Figure 14 displays the nondifferentiated AES features of a GaN sample. As the exposure time to N_2/He plasma increased, Ga *LMM* (~1058.5 eV) and O *KLL* (~505.0 eV) features of the oxide film gradually shift to higher energy. Figure 15 shows the atomic fractions of each element, [Ga], [O], and [N]. Although [Ga] shows negligible change from the initial concentration of ~50 at. %, [N] and [O] saturate at ~25 at. % with increasing nitridation time.

E. Interface quality of GaN MOS system

The impacts of RPAO oxide thickness and nitrogen incorporation on the quality of the interface and dielectric layer were investigated using test GaN metal-oxide-semiconductor (MOS) capacitors. From the relation of oxide thickness versus oxidation time shown in Fig. 5, the RPAO process using O_2 source gas was performed for 30 s (or 180 s) to obtain a thin ~1.0 nm (or ~1.6 nm) RPAO oxide. For the nitrogen-incorporated RPAO oxide, GaN MOS samples were prepared by the (i) RPAO process using 1% N_2O in N_2 source gas, and (ii) RPAO process using O_2 source gas followed by ni-

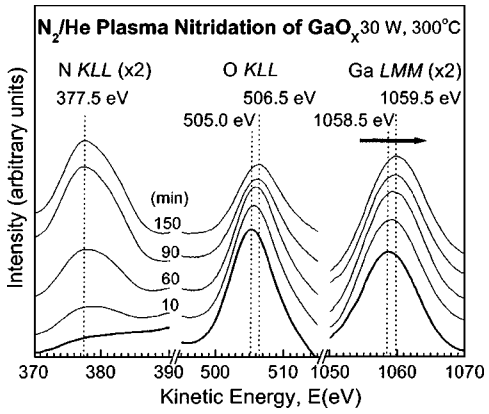

FIG. 14. Time evolution of nondifferential AES spectra from O_2/He-plasma-oxidized GaN sample (GaO_x, ~3.5 nm) and N_2/He-plasma-nitridation processing of GaO_x.

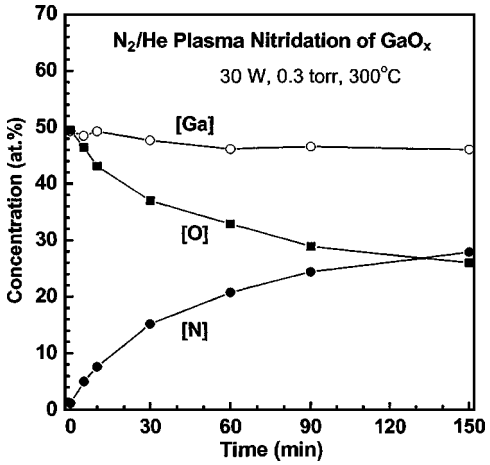

FIG. 15. Relative change in composition of GaO_x as a function of nitridation time, where [Ga], [O], and [N] are Ga, O, and N atomic fraction in the film (at. %), respectively.

tridation using N_2/He plasma at 0.3 Torr for 90 s. To control the thickness at ~1 nm of RPAO oxide using 1% N_2O in N_2 source gas, the RPAO process was performed for 600 s, as shown in Fig. 11. In this section, the characterization of each GaN MOS sample focused on the interface-trapped charge (Q_{it}), rather than the oxide fixed charge (Q_f) because the extraction of Q_f from the flat-band voltage shift (ΔV_{fb}) has several uncertainties, such as the (i) compensated effect[24] between Q_f and Q_{it}, and (ii) uncertain doping concentration of the GaN MOS system, which was usually obtained from a close fit of the capacitance-voltage (*C-V*) curve. The exact evaluation of Q_f using ΔV_{fb} is possible after minimizing Q_{it}.

Figures 16 and 17 show the frequency dependence of *C-V* characteristics of GaN MOS capacitors. The gate voltage was swept from positive to negative voltage at room temperature in the dark, and frequencies were 3, 10, and 100 kHz and 1 MHz. To determine D_{it} of each GaN MOS sample, the high-low frequency method was applied to measured *C-V* curves. *C-V* curves measured at 1 MHz and 3 kHz were used as high- and low-frequency *C-V* curves, respectively. The minimum D_{it} of each GaN MOS capacitor was determined at the gate voltage, where measured *C-V* curves at 3 kHz and 1 MHz showed the maximum capacitance difference (ΔC_{max}). Note that the actual D_{it} will be higher than the estimated value using this method. Using the *C-V* curves at 3 kHz and 1 MHz, D_{it} is calculated from[25]

$$D_{it} = \frac{C_{ox}}{q}\left(\frac{C_{lf}/C_{ox}}{1 - C_{lf}/C_{ox}} - \frac{C_{hf}/C_{ox}}{1 - C_{hf}/C_{ox}}\right). \quad (5)$$

Figure 18 shows the minimum D_{it} of each GaN MOS capacitor determined at the gate voltage of ΔC_{max}. By increasing the thickness of RPAO oxide from (i) ~1.0 nm to (ii) ~1.6 nm, D_{it} increased from $\sim 6\times10^{11}$ to 9×10^{11} $cm^{-2}\,eV^{-1}$, respectively. Considering the sample using 1% N_2O in N_2 source gas performed for 600 s, it is reasonable to conclude that this increased D_{it} is caused by the increased thickness of RPAO oxide, rather than by possible plasma-induced damage. The lowest value of D_{it}, ~4

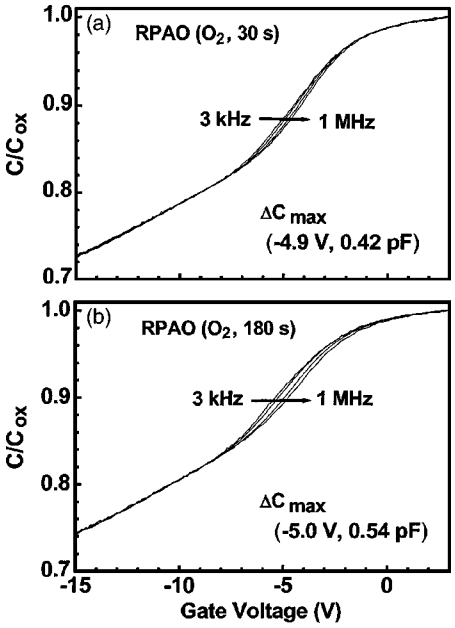

FIG. 16. Frequency dependence (3, 10, and 100 kHz and 1 MHz) of the *C-V* characteristics of GaN MOS capacitors. The RPAO process using O_2 source gas was performed for (a) 30 s to obtain thin RPAO oxide of ~1.0 nm, and (b) 180 s to obtain thin RPAO oxide of ~1.6 nm. The minimum D_{it} of each GaN MOS capacitor was determined at the gate voltage where measured *C-V* curves at 3 kHz and 1 MHz showed the maximum capacitance difference (ΔC_{max}).

$\times10^{11}$ $cm^{-2}\,eV^{-1}$, was obtained by the RPAO process using O_2 source gas, followed by nitridation using N_2/He plasma. The small decrease using the N_2O source gas is consistent with results obtained for Si-SiO_2 devices, where the RPAO process was used.[17] The changes in D_{it} between using O_2 and

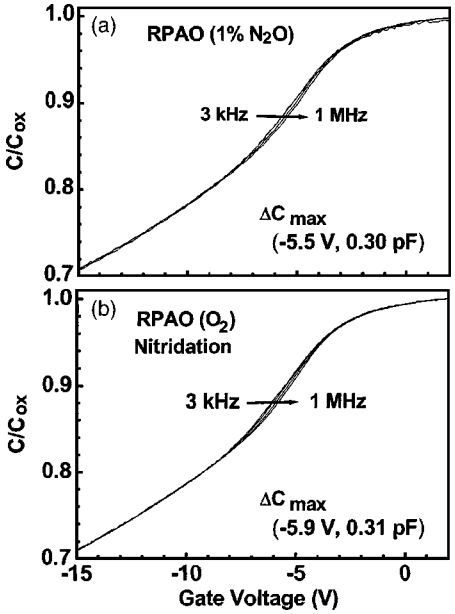

FIG. 17. Frequency dependence (3, 10, and 100 kHz and 1 MHz) of the *C-V* characteristics of GaN MOS capacitors: (a) RPAO process using 1% N_2O in N_2 source gas, and (b) RPAO process using O_2 source gas, followed by nitridation using N_2/He plasma.

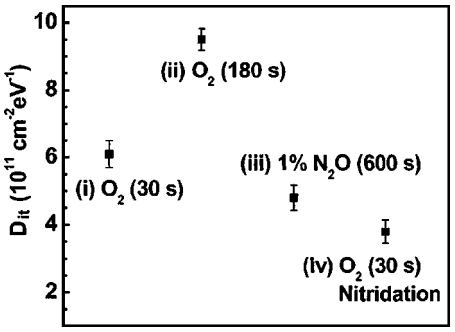

FIG. 18. Minimum density of interface state (D_{it}) of GaN MOS capacitors with RPAO process using (i) O_2 source gas for 30 s, (ii) O_2 source gas for 180 s, (iii) 1% N_2O in N_2 source gas for 600 s, and (iv) O_2 source gas for 30 s, followed by nitridation using N_2/He plasma for 90 s.

N_2O are outside the range of experimental uncertainty, but are really too small to be useful compared to the more significant decrease in D_{it} using an optimized post oxidation, plasma nitridation step.

IV. CONCLUSION

Remote plasma-assisted oxidation of a GaN surface using O_2, N_2O, and 10% (or 1%) N_2O in N_2 source gas has been investigated as the first step for the independent control of the GaN-GaO_x (or GaO_xN_y) interface formation and dielectric film deposition. The initial oxidation kinetics and chemical composition of thin oxide are determined from analysis of on-line AES features associated with Ga, N, and O. The plasma-assisted oxidation process is self-limiting with power-law kinetics similar to those for the plasma-assisted oxidation of Si and SiC. Oxidation using O_2/He plasma forms nearly pure GaO_x, and oxidation using 1% N_2O in N_2 forms GaO_xN_y with small nitrogen content, $\sim 4-7$ at. %. The impacts were investigated of RPAO oxide thickness and nitrogen incorporation on the interface and dielectric layer quality, and the lowest value of the interface state density, $\sim 4\times 10^{11}$ cm^{-2} eV^{-1}, was obtained by the RPAO process using O_2 source gas to form ~ 1.0 nm of RPAO oxide, followed by nitridation using N_2/He plasma. The control of RPAO oxide as a superficially thin (or several monolayer) oxide and enhancement of incorporated nitrogen content are essential requirements to reduce the interface state density of GaN MOS systems.

ACKNOWLEDGMENTS

This research is supported by the ONR, AFOSR, SRC, and i-Sematech/SRC Front End Processes Center.

[1] S. J. Pearton, F. Ren, A. P. Zhang, and K. P. Lee, Mater. Sci. Eng., R. **30**, 55 (2000).
[2] H. C. Casey, G. G. Fountain, R. G. Alley, B. P. Keller, and S. P. DenBaars, Appl. Phys. Lett. **68**, 1850 (1996).
[3] S. Arulkumaran, T. Egawa, H. Ishikawa, T. Jimbo, and M. Umeno, Appl. Phys. Lett. **73**, 809 (1998).
[4] L. W. Tu, W. C. Kuo, K. H. Lee, P. H. Tsao, C. M. Lai, A. K. Chu, and J. K. Sheu, Appl. Phys. Lett. **77**, 4 (2000).
[5] E. Alekseev, A. Eisenbach, and D. Pavlidis, Electron. Lett. **35**, 2145 (1999).
[6] J. W. Johnson, B. Luo, F. Ren, B. P. Gila, W. Krishnamoorthy, C. R. Abernathy, S. J. Pearton, J. I. Chyi, T. E. Nee, C. M. Lee, and C. C. Chuo, Appl. Phys. Lett. **77**, 3230 (2000).
[7] M. Hong, K. A. Anselm, J. Kwo, H. M. Ng, J. N. Baillargeon, A. R. Kortan, C. M. Lee, J. I. Chyi, and T. S. Lay, J. Vac. Sci. Technol. B **18**, 1453 (2000).
[8] S. D. Wolter, B. P. Luther, D. L. Waltemyer, C. Önneby, S. E. Mohney, and R. J. Molnar, Appl. Phys. Lett. **70**, 16, 2156 (2000).
[9] H. Kim, S. J. Park, and H. Hwang, J. Vac. Sci. Technol. B **19**, 579 (2001).
[10] L.-H. Peng, C.-H. Liao,Y.-C. Hsu, C.-S. Jong, C.-N. Huang, J.-K. Ho, C.-C. Chiu, and C.-Y. Chen, Appl. Phys. Lett. **76**, 4, 511 (2000).
[11] T. Rotter, R. Ferretti, D. Mistele, F. Fedler, H. Klausing, J. Stemmer, O. K. Semchinova, J. Aderhold, and J. Graul, J. Cryst. Growth **230**, 602 (2001).
[12] D. J. Fu, Y. H. Kwon, T. W. Kang, C. J. Park, K. H. Baek, H. Y. Cho, D. H. Shin, C. H. Lee, and K. S. Chung, Appl. Phys. Lett. **80**, 3, 446 (2002).
[13] R. Therrien, G. Lucovsky, and R. Davis, Appl. Surf. Sci. **166**, 513 (2000).
[14] H. Kim, N. M. Park, J. S. Jang, S. J. Park, and H. Hwang, Electrochem. Solid-State Lett. **4**, G104 (2001).
[15] B. Gaffey, L. J. Guido, X. W. Wang, and T. P. Ma, IEEE Trans. Electron Devices **48**, 458 (2001).
[16] T. Yasuda, Y. Ma, S. Habermehl, and G. Lucovsky, Appl. Phys. Lett. **60**, 434 (1992).
[17] G. Lucovsky, IBM J. Res. Dev. **43**, 301 (1999).
[18] A. Gölz, G. Lucovsky, K. Koh, D. Wolfe, H. Niimi, and H. Kurz, J. Vac. Sci. Technol. B **15**, 1097 (1997).
[19] J. Kwo, D. W. Murphy, M. Hong, R. L. Opila, J. P. Mannaerts, A. M. Sergent, and R. L. Masaitis, Appl. Phys. Lett. **75**, 1116 (1999).
[20] M. Hong, J. Kwo, A. R. Kortan, J. P. Mannaerts, and A. M. Sergent, Science **283**, 1897 (1999).
[21] S. Pal, S. K. Ray, B. R. Chakraborty, S. K. Lahiri, and D. N. Bose, J. Appl. Phys. **90**, 4103 (2001).
[22] C. Bae and G. Lucovsky, Surf. Sci. **532–535**, 759 (2003).
[23] H. Nimi, *Monolayer-Level Controlled Incorporation of Nitrogen in Ultra-Thin Gate Dielectrics using Remote Plasma Processing*, Ph.D. thesis, North Carolina State University (1998), p. 223.
[24] J. A. Cooper, Jr., Phys. Status Solidi A **162**, 305 (1997).
[25] D. K. Schroder, *Semiconductor Material and Device Characterization*, 2nd ed. (Wiley, New York, 1998), p. 371.